

Liquid-Crystalline Polymers Containing Mesogenic Units Based on Half-Disk and Rodlike Moieties. 5. Side-Chain Liquid-Crystalline Poly(methylsiloxanes) Containing Hemiphasmidic Mesogens Based on 4-[[3,4,5-Tris(alkan-1-yloxy)benzoyl]oxy]-4'-[[p-(propan-1-yloxy)benzoyl]oxy]biphenyl Groups

V. Percec* and J. Heck

Department of Macromolecular Science, Case Western Reserve University, Cleveland, Ohio 44106

G. Ungar

School of Materials, The University of Sheffield, Sheffield, S10 2TZ, U.K.

Received February 7, 1991; Revised Manuscript Received April 3, 1991

ABSTRACT: The synthesis of hemiphasmidic monomers 4-[[3,4,5-tris[(S)-(-)-2-methylbutan-1-yl]oxy]benzoyl]oxy]-4'-[[p-(allyloxy)benzoyl]oxy]biphenyl (14), 4-[[3,4,5-tris(n-pentan-1-yloxy)benzoyl]oxy]-4'-[[p-(allyloxy)benzoyl]oxy]biphenyl (15), and 4-[[3,4,5-tris(n-dodecan-1-yloxy)benzoyl]oxy]-4'-[[p-(allyloxy)benzoyl]oxy]biphenyl (16) and of the corresponding poly(methylsiloxanes) (17-19) is described. Both monomers and polymers were characterized by a combination of DSC, WAXS, SAXS, and thermal optical polarized microscopy. 15-17 are crystalline. 17 exhibits an enantiotropic double-layer smectic A or C mesophase. 18 displays a monotropic columnar hexagonal and an enantiotropic double-layer smectic A or C mesophases. Due to its close proximity to the glass transition temperature, the columnar hexagonal phase of 18 is strongly kinetically controlled. 19 exhibits a very broad enantiotropic hexagonal columnar mesophase. The columns of the mesophases of 18 and 19 are generated by an elongated polymer backbone penetrating through the center of the column and tapered extended mesogens radiating out of it.

Introduction

Previous publications from both our¹⁻⁵ and Ringsdorf's⁶ laboratories have reported on the synthesis of polymers containing mesogenic units that represent a combination of half-disk and rodlike moieties.⁷

Low molar mass liquid crystals based on various combinations of half-disk and rodlike moieties represent a novel class of liquid crystals.⁷⁻¹⁴ Combinations of two half-disks and a rodlike moiety are known as phasmidic liquid crystals or phasמידs, while combinations of a half-disk and a rodlike moiety are known as hemiphasמידs.⁷ Low molar mass phasמידs and hemiphasמידs form either columnar hexagonal (Φ_h)⁸⁻¹³ or biaxial nematic (N_b)¹⁴⁻¹⁶ mesophases.

Although hexagonal columnar mesophases are frequently obtained from flexible or rigid disklike mesogens or polymers containing disklike mesogens,^{16,17} there are many examples of conventional flexible polymers that exhibit columnar hexagonal mesophases.^{17f} A recent example of a flexible polymer that displays a hexagonal columnar mesophase was provided by a nondiscotic copolyether based on 1,2-bis(4-hydroxyphenyl)ethane, 1,8-dibromooctane, and 1,12-dibromododecane.¹⁸ In addition, lyotropic hexagonal columnar mesophases are traditionally formed by surfactants.¹⁹

We believe that hemiphasמידs and related structures can map the borderline between rigid and flexible, disklike and rodlike, thermotropic and lyotropic, as well as other nonconventional and conventional molecules that display hexagonal columnar mesophases. Consequently, on one side polymers containing hemiphasמידic mesogens are of interest since they can bridge between these multiple mesogenic architectures. On the other side they may provide an entry to the molecular understanding and

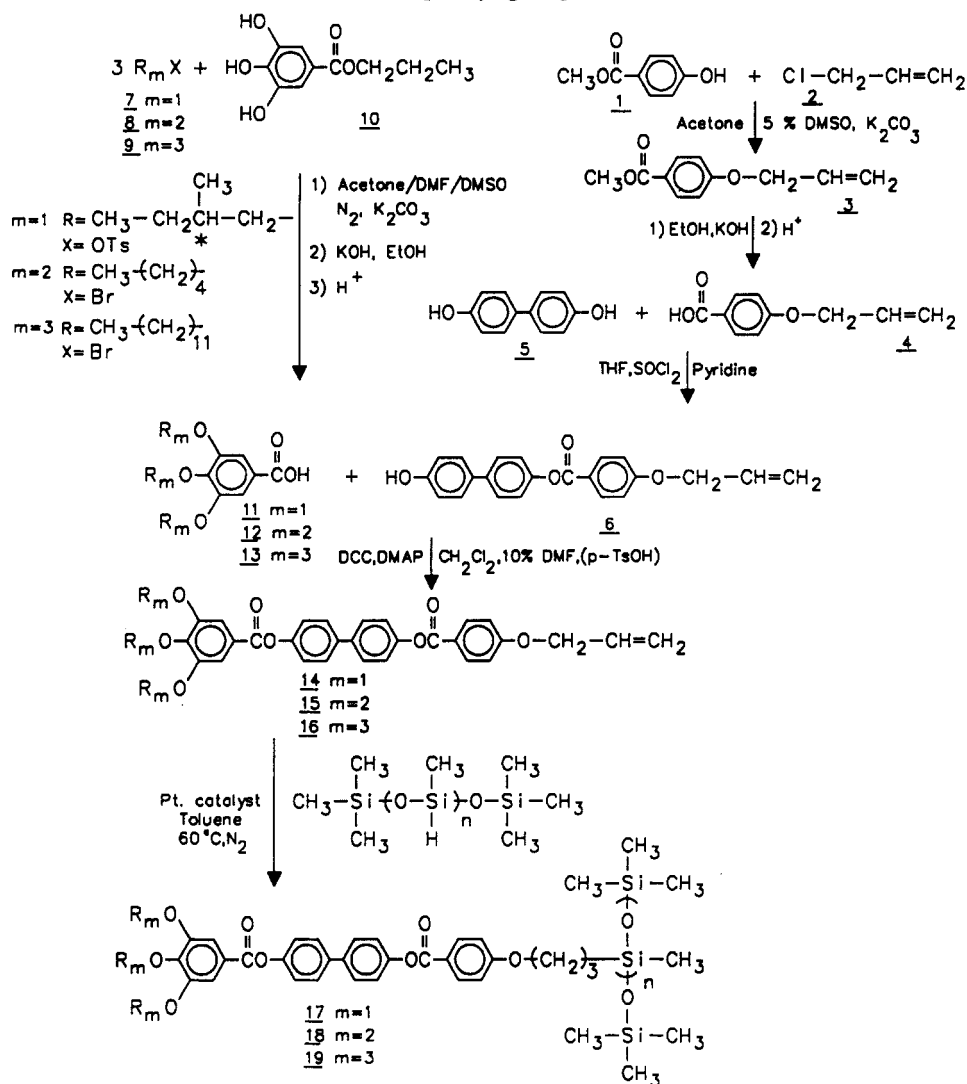
design of novel supramolecular polymer architectures by using more conventional synthetic approaches.

The goal of this paper is to describe the synthesis and characterization of the hemiphasמידic monomers 4-[[3,4,5-tris[(S)-(-)-2-methylbutan-1-yl]oxy]benzoyl]oxy]-4'-[[p-(allyloxy)benzoyl]oxy]biphenyl (14), 4-[[3,4,5-tris(n-pentan-1-yloxy)benzoyl]oxy]-4'-[[p-(allyloxy)benzoyl]oxy]biphenyl (15), and 4-[[3,4,5-tris(n-dodecan-1-yloxy)benzoyl]oxy]-4'-[[p-(allyloxy)benzoyl]oxy]biphenyl (16), and of the poly(methylsiloxanes) derived from them (i.e., 17-19).

Experimental Section

Materials. Propyl 3,4,5-trihydroxybenzoate (97%, Aldrich), methyl p-hydroxybenzoate (99%, Aldrich), 4,4'-dihydroxybiphenyl (97%, gift from Amoco), 1-bromopentane (99%, Aldrich), 1-bromododecane (98%, Aldrich), (S)-(-)-2-methyl-1-butanol (95%, Fluka), 4-(dimethylamino)pyridine (DMAP) (98%, Fluka), allyl chloride (98%, Aldrich), SOCl_2 , and the other conventional reagents were used as received. Tetrahydrofuran (THF) was distilled from LiAlH_4 . CH_2Cl_2 was distilled from CaH_2 . Dimethyl sulfoxide (DMSO) and dimethylformamide (DMF) were stirred overnight at 100 °C over CaO and then distilled from CaO under vacuum. Pyridine was heated overnight at 100 °C over KOH , distilled from KOH , and then stored over KOH . 1,3-Dicyclohexylcarbodiimide (DCC, 99%, Aldrich) was dissolved in hexanes and filtered and the solvent evaporated. p-Toluene-sulfonic acid (p-TsOH, 98%, Aldrich) was dried in a desiccator under vacuum for 24 h. The poly(methylsiloxane) ($M_n = 1500$ as reported by Petrarch, $M_n = 2700$ as determined by 200-MHz ^1H NMR spectroscopy) was used as received. Toluene and xylene were both washed with 50-mL portions of H_2SO_4 until the portions were relatively uncolored, washed with water until neutral pH, dried over MgSO_4 , filtered, allowed to reflux overnight over Na, and then distilled from Na. The platinum divinyltetramethyldisiloxane catalyst (solution in xylene from Petrarch) was purified by placing it in a clean flamed-dried round-bottom

Scheme I
Synthesis of Poly(methylsiloxanes) Based on 4-[[3,4,5-Tris(alkan-1-yloxy)benzoyl]oxy]-4'-[[p-(allyloxy)benzoyl]oxy]-biphenyl groups



flask with gas inlet adapter, which was attached to a vacuum line (0.2 mmHg). A beaker of warm tap water was placed under the flask so as to partially submerge it. The tap water was replaced as it cooled and the vacuum maintained for 8 h, after which the remaining catalyst was diluted to 30 times its original volume with the previously dried xylene, sealed, and stored in a desiccator. The benzoic acids and phenols used in the esterifications and the monomers used in hydrosilations were dried under vacuum in a desiccator for 24 h prior to use.

Techniques. ^1H NMR (200-MHz) spectra were recorded on a Varian XL-200 spectrometer. Infrared (IR) spectra were recorded on a Perkin-Elmer 1320 infrared spectrometer. Relative molecular weights of polymers were measured by gel permeation chromatography (GPC) with a Perkin-Elmer Series 10 LC instrument equipped with an LC-100 column oven and a Nelson 900 series integrator data station. A set of two Polymer Laboratories PL gel columns of 5×10^2 and 10^4 Å with CHCl_3 as solvent (1 mL/min) was used. The measurements were made at 40°C with the UV detector. Polystyrene standards were used for the calibration plot. High-pressure liquid chromatography (HPLC) experiments were performed with the same instrument. A Perkin-Elmer DSC-4 differential scanning calorimeter equipped with a TADS data station was used to determine the thermal transitions, which were reported as the maximum and minimum of their endothermic and exothermic peaks. In all cases, heating and cooling rates were $20^\circ\text{C}/\text{min}$ unless specified. Glass transition temperatures (T_g) were read at the middle of the change in heat capacity. First heating scans differ from second and subsequent heating scans. However, second and subsequent heating scans are identical. The difference between various DSC scans will be discussed. X-ray scattering patterns were recorded

with either a flat plate wide-angle (WAXS) vacuum camera (room temperature and elevated temperatures) or a pinhole collimated small-angle (SAXS) camera (room temperature). Ni-filtered $\text{Cu K}\alpha$ radiation was used. The samples were in the form of (a) as-prepared polymers in the form of a free-standing powder or (b) bulk samples in Lindemann capillaries cooled from the melt. The temperature stability of the X-ray heating cell was $\pm 0.1^\circ\text{C}$. A Carl-Zeiss optical polarized microscope (magnification $100\times$) equipped with a Mettler FP82 hot stage and a Mettler FP800 central processor was used to observe the thermal transitions and to analyze the anisotropic textures.

Synthesis of the Monomers and Polymers. Monomers and polymers were synthesized as outlined in Scheme I.

The synthesis, purification, and characterization of methyl *p*-(allyloxy)benzoate (3), *p*-(allyloxy)benzoic acid (4), 4-hydroxy-4'-[[*p*-(allyloxy)benzoyl]oxy]biphenyl (6), 4-(*S*)-(-)-2-methyl-1-butyl tosylate (7),^{5,20} 3,4,5-tris[(*S*)-(-)-2-methylbutan-1-yl]oxy]benzoic acid (11),⁵ 3,4,5-tris(*n*-pentan-1-yloxy)benzoic acid (12),⁵ and 3,4,5-tris(*n*-dodecan-1-yloxy)benzoic acid (13)⁵ were described in previous publications from our laboratory.

Synthesis of 4-[[3,4,5-Tris[(*S*)-(-)-2-methylbutan-1-yl]oxy]benzoyl]oxy]-4'-[[*p*-(allyloxy)benzoyl]oxy]biphenyl (14). A solution of 1.58 g (4.1 mmol) of 3,4,5-tris[(*S*)-(-)-2-methylbutan-1-yl]oxy]benzoic acid (11), 1.45 g (4.2 mmol) of 4-hydroxy-4'-[[*p*-(allyloxy)benzoyl]oxy]biphenyl (6), 0.85 g (4.1 mmol) of DCC, 0.1 g (1 mmol) of DMAP, and 0.1 g (1 mmol) of *p*-TsOH²¹ in a mixture of 50 mL of dry CH_2Cl_2 containing 10% dry DMF was stirred at room temperature for 16 h. The resulting precipitate was filtered, and the CH_2Cl_2 was evaporated in a rotary evaporator. THF (20 mL) and H_2O (1 mL) were added and the solution was allowed to stir for 1 h. The mixture was

poured into 200 mL of H₂O, and the product was extracted with CH₂Cl₂. The volume of the CH₂Cl₂ was reduced on the rotary evaporator, and the solution was precipitated into 10 times excess of methanol (MeOH). The resulting precipitate was filtered and allowed to dry in air. The product was purified by flash chromatography (basic alumina, CH₂Cl₂ eluent), the volume of the CH₂Cl₂ was reduced on the rotary evaporator, and the solution was precipitated into MeOH. The precipitate was filtered and dried yielding 1.02 g (35%) of a white solid. Purity: 99% (HPLC). mp: 143 °C Differential scanning calorimetry (DSC, 20 °C/min). ¹H NMR (CDCl₃, TMS, δ, ppm): 0.96 (t, 9 H, CH₃CH₂-CH*), 1.06 (d, 9 H, CH₃CH*), 1.31, 1.61, 1.91 (3 m, 9 H, CH₃CH₂CH*), 3.90 (overlapped t, 6 H, CH₂O), 4.64 (d, 2 H, CH₂-CH=CH₂), 5.37 (d, 1 H, CH=CH₂ trans), 5.44 (d, 1 H, CH=CH₂ cis), 6.08 (m, 1 H, CH=CH₂), 7.01 (d, 2 H, CH₂=CHCH₂-OPhHCOO ortho from O), 7.29 (d, 4 H, biphenyl ortho from OOC), 7.42 (s, 2 H, PhHCOO), 7.63 (d, 4 H, biphenyl meta from OOC), 8.17 (d, 2 H, CH₂=CHCH₂-OPhHCOO meta from O). IR (KBr plate): 1720 cm⁻¹ (ν_{C=O}).

Synthesis of 4-[[3,4,5-Tris(*n*-pentan-1-yloxy)benzoyl]oxy]-4'-[[*p*-(allyloxy)benzoyl]oxy]biphenyl (15). Compound 15 was synthesized and purified according to the same procedure as the one used for the preparation of 14 except that the esterification was performed in the absence of *p*-TsOH, and the precipitations in MeOH were done at a temperature of <-10 °C. A 2.2-g (5.8 mmol) aliquot of 3,4,5-tris(*n*-pentan-1-yloxy)benzoic acid (12) and 2.0 g (5.8 mmol) of 4-hydroxy-4'-[[*p*-(allyloxy)benzoyl]oxy]biphenyl (6) were used to obtain 1.02 g (25%) of a white solid. Purity: 99% (HPLC). mp: 93 °C (DSC, 20 °C/min). ¹H NMR (CDCl₃, TMS, δ, ppm): 0.97 (t, 9 H, CH₃), 1.46 (m, 12 H, (CH₂)₄), 1.83 (m, 6 H, CH₂CH₂OPh), 4.06 (overlapped t, 6 H, CH₂CH₂OPh), 4.63 (d, 2 H, CH₂CH=CH₂), 5.34 (d, 1 H, CH=CH₂ trans), 5.42 (d, 1 H, CH=CH₂ cis), 6.07 (m, 1 H, CH=CH₂), 7.00 (d, 2 H, CH₂=CHCH₂-OPhHCOO ortho from O), 7.28 (d, 4 H, biphenyl ortho from OOC), 7.43 (s, 2 H, PhHCOO), 7.63 (d, 4 H, biphenyl meta from OOC), 8.17 (d, 2 H, CH₂=CHCH₂-OPhHCOO meta from O). IR (KBr plate): 1715 cm⁻¹ (ν_{C=O}).

Synthesis of 4-[[3,4,5-Tris(*n*-dodecan-1-yloxy)benzoyl]oxy]-4'-[[*p*-(allyloxy)benzoyl]oxy]biphenyl (16). Compound 16 was synthesized and purified according to the same procedure as the one used for the preparation of 14. A 1.5-g (2.2 mmol) aliquot of 3,4,5-tris(*n*-dodecan-1-yloxy)benzoic acid (13) and 0.8 g (2.3 mmol) of 4-hydroxy-4'-[[*p*-(allyloxy)benzoyl]oxy]biphenyl (6) were used to obtain 1.6 g (71%) of a white solid. Purity: 98% (HPLC). mp: 91 °C (DSC, 20 °C/min). ¹H NMR (CDCl₃, TMS, δ, ppm): 0.85 (t, 9 H, CH₃), 1.27 (m, 54 H, (CH₂)₁₀), 1.77 (m, 6 H, CH₂CH₂OPh), 4.03 (t, 6 H, CH₂O), 4.60 (d, 2 H, CH₂-CH=CH₂), 5.36 (d, 1 H, CH=CH₂ trans), 5.43 (d, 1 H, CH=CH₂ cis), 6.08 (m, 1 H, CH=CH₂), 6.99 (d, 2 H, CH₂=CHCH₂-OPhHCOO ortho from O), 7.25 (d, 4 H, biphenyl ortho from OOC), 7.40 (s, 2 H, PhHCOO), 7.61 (d, 4 H, biphenyl meta from OOC), 8.14 (d, 2 H, CH₂=CHCH₂-OPhHCOO meta from O). IR (KBr plate): 1715 cm⁻¹ (ν_{C=O}).

Synthesis of Poly(methylsiloxanes) (17–19). The poly(methylsiloxanes) 17–19 were synthesized by the hydrosilation of monomers 14–16 with a poly(hydrogenmethylsiloxane). A general method for their preparation and purification is described below: To a flame-dried 5-mL test tube containing a microstirring bar were added 0.60 g (0.85 mmol) of 15, 0.050 g (0.83 mmol) of poly(hydrogenmethylsiloxane), 2–3 mL of dry toluene, and five drops (~0.1 g) of purified platinum divinyltetramethyldisiloxane complex. The reaction was purged with nitrogen and the tube was sealed with a cork stopper covered with Teflon tape. The reaction mixture was heated for 24 h at 60 °C, after which 0.04 g (0.4 mmol) of 1-octene and two additional drops (~0.04 g) of catalyst were added and the reaction was continued at 60 °C for 2 h. The solution was then cooled and precipitated into methanol. The precipitate was filtered, dissolved in CH₂Cl₂, and precipitated in acetone cooled to <-10 °C, filtered, and dried to yield 0.13 g (22%) of a white solid. Purity: 99% (HPLC). *M_n* = 20 000, *M_w*/*M_n* = 1.6 (GPC). The analysis of all polymers by ¹H NMR showed no detectable incorporation of 1-octene into the polymer structure. Nevertheless, the addition of 1-octene was used in all cases in order to prevent the presence of any unreacted SiH groups in the final polymers.

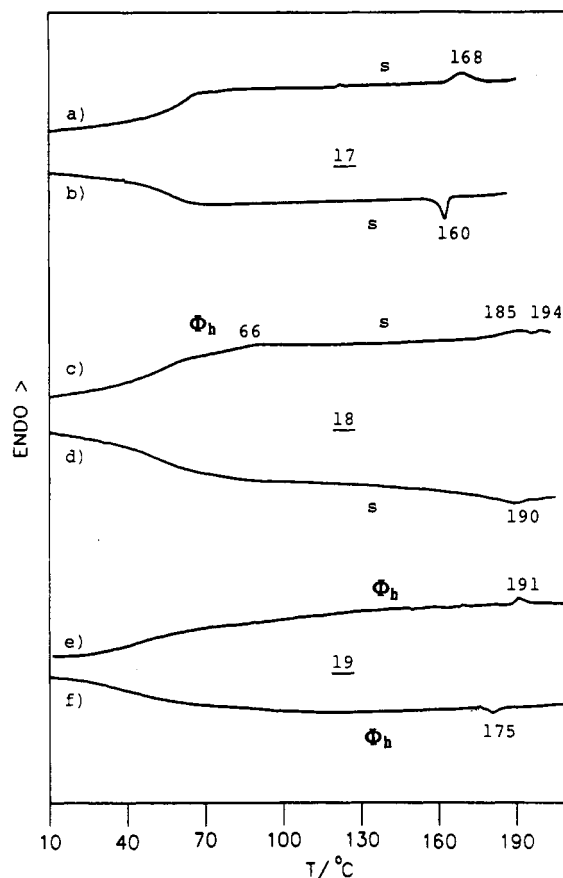


Figure 1. Heating and cooling DSC traces of 17 (a) second heating scan and (b) first cooling scan, 18 (c) second heating scan and (d) first cooling scan, and 19 (e) second heating scan and (f) first cooling scan.

Results and Discussion

The synthesis of monomers 14–16 and of polymers 17–19 is described in Scheme I and is based on a modified reaction scheme that was used for the preparation of other polymers containing hemiphasmic mesogens.^{1–5} The characterization of both monomers and polymers was performed by a combination of DSC, WAXS, SAXS, and thermal optical polarized microscopy. Monomers 14–16 are only crystalline. As predicted on the basis of thermodynamic assumptions,²² and observed experimentally,²³ upon polymerization virtual and monotropic mesomorphic phase-transition temperatures of monomers became enantiotropic. This has also been the case for side-chain liquid-crystalline polymers containing hemiphasmic mesogens synthesized previously in our laboratory.^{1–5}

Figure 1 presents the DSC traces of the second heating scan and of the first cooling scan of polymers 17–19. In the case of polymers 18 and 19, the first DSC heating scans are slightly different from second scans. However, second and subsequent heating scans and first and subsequent cooling scans are identical. Phase-transition temperatures collected from first and second heating and from the first cooling DSC scans are summarized in Table I.

First, second, and subsequent heating DSC scans of polymer 17 are identical (Figure 1a and Table I). Polymer 17 exhibits an enantiotropic mesophase. X-rays scattering experiments, which will be discussed in the latter part of this paper, have shown that the mesophase of 17 is of smectic type. This mesophase is characterized by a very low isotropization enthalpy (Table I). The isotropic-smectic phase-transition temperature of 17 exhibits only a low degree of supercooling.

Table I
Characterization of Polysiloxanes 17–19^a

polym	M_n^b	M_w/M_n^b	purity, ^c %	yield, %	phase transitions, °C (corres enthalpy changes, kcal/mru) ^d	
					heating	cooling
17	21 000	1.4	99	53	g 59 s 168 (0.11) i g 60 s 168 (0.11) i	i 160 (0.11) s 54 g
18	20 000	1.6	99	22	g 48 Φ_h 66 (1.0) s 193 (0.08) i g 49 Φ_h 66 (0.09) s 185, 194 (0.06) ^e i	i 190, 182 (0.11) ^e s 49 g
19	23 000	1.7	98	55	g 48 Φ_h 126 (3.0) Φ_h 193 (0.4) i g 40 Φ_h 191 (0.08) i	i 175 (0.06) Φ_h 33 g

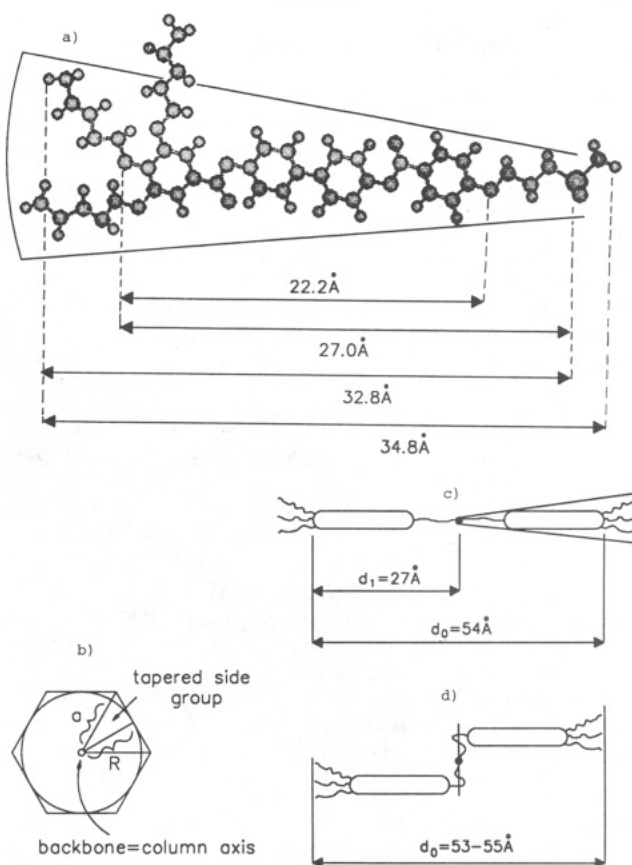
^a (g, glassy phase, Φ_h , hexagonal columnar mesophase, s, smectic mesophase, i, isotropic: data on the first line for each polymer are from the first heating and cooling scans, data on the second line are from the second heating scan). ^b By GPC. ^c By HPLC. ^d mru, mole repeat unit. ^e Combined enthalpy for overlapped transitions.

Polymer 18 displays multiple phase transitions on its heating and cooling DSC scans (Figure 1c,d). On the first heating scan, above the glass transition temperature, 18 exhibits a hexagonal columnar (Φ_h) mesophase, which changes at 66 °C into a smectic phase (see further discussion on X-ray scattering experiments). The smectic phase undergoes isotropization at 193 °C (Table I). The main difference between the first and second heating DSC scans consists of the lower enthalpy associated with the $\Phi_h \rightarrow s$ phase transition at 66 °C in the second heating scan (Table I). In addition, the isotropization peak at 193 °C in the first heating scan gets split into two peaks in the second DSC heating scan (185 and 194 °C). X-ray scattering experiments, which will be discussed later, showed that there is no phase change associated with the peak at 185 °C. On cooling from the isotropic phase, polymer 18 shows only an isotropic–smectic phase transition at 190 °C. We can speculate that the Φ_h phase of this polymer is strongly controlled by kinetics due to its close proximity to the glass transition temperature of the polymer. This assumption was confirmed by X-ray scattering experiments and is in agreement with similar results observed on other side-chain liquid-crystalline polymers reported from our laboratory.²⁴

In the first DSC heating scan polymer 19 presents an endotherm at 126 °C followed by an isotropization transition at 193 °C (Table I). In the first heating scan X-ray scattering experiments showed the generation of the Φ_h mesophase above the peak at 126 °C. Below this peak, the polymer shows only one broad peak in the SAXS curve, which sharpens up above this temperature to become the 100_{hex} peak. What actually happens is that the “endotherm” from 126 °C appears to be associated with the glass transition so that an amorphous as-precipitated polymer becomes a well-ordered columnar hexagonal phase at that temperature. On the second and subsequent heating and first and subsequent cooling DSC scans, polymer 19 exhibits an enantiotropic hexagonal columnar mesophase (Figure 1e,f).

The assignment of the mesophases of polymers 17–19 was performed by X-ray scattering experiments. Discrimination between smectic (s) and hexagonal columnar (Φ_h) mesophases relies on the presence (in the case of Φ_h) or the absence (in the case of s) of an X-ray reflection with $d = d_0/(3)^{1/2}$ in addition to the $d = d_0/2$ reflection, which is present in both Φ_h and s phases [where d_0 is the basic intense reflection, i.e., 001 (in the case of s) or 100 (in the case of Φ_h)]. In the absence of oriented samples all but d_0 rings are weak. No wide-angle reflection is observed in any polymer at any temperature. Only a diffuse halo centered at a Bragg spacing of 4.5 Å is observed. This indicates that none of these polymers display crystalline phases.

The low-temperature phase of the thermally untreated polymer 18 (i.e., powder separated by precipitation, above its glass transition temperature) is characterized by $d_0 =$

Chart I^a

^a (a) Planar tapered extended conformation of the structural unit of polymer 18; (b) top view of a column from the hexagonal columnar phase (Φ_h) exhibited by polymers 18 and 19; (c) the double-layer smectic structure of 18 with an extended spacer (too large); (d) the double-layer smectic structure of 18 with coiled spacer.

$46.5 \text{ Å (strong)} = d_{100}^{\text{hex}}$, $d_1 = 26.5 (\pm 0.5) \text{ Å (weak)} = d_{100}^{\text{hex}}$ ($d_1/d_0 = 1.75 \approx 3^{1/2}$). No d_{220}^{hex} reflection could be discerned, and the widths of both observed diffraction maxima suggest relatively poor order. Annealing at temperatures significantly above T_g could not be performed due to the phase transition taking place around 66 °C (Figure 1c). From the observed 100 and 110 diffraction peaks, the radius of the column is calculated as $R = d_{100}/(3)^{1/2} = 27 \text{ Å}$ and its diameter $2R$ as 54 Å . Let us compare the experimental value of R with the length of the extended conformation of the molecular model of the planar tapered shape of the structural unit of 18 (Chart Ia). This value calculated from the Si atom to the hydrogen end is 32.8 Å , and after including the van der Waals radius of hydrogen, it becomes 34 Å . Chart I shows a projection down the column that assumes that each column occupies a hexagonal cross section. From Chart Ib, $a = (2/3^{1/2})R = 31 \text{ Å}$.

According to these data, it seems reasonable to assume that the polymer backbone is located in the center of the column. The hemiphasmidic tapered side groups are radiating out of the center of the column. Both R and a values from Chart Ib are less than the extended conformation of the side groups, i.e., 34 Å. This difference can be explained by (a) a contraction of the pentyl tails, (b) a contraction of the propyl space, or (c) an interdigitation of the pentyl tails from the neighboring columns. A discrimination between these three possibilities is not yet possible.

Upon heating above the endotherm at 66 °C (Figure 1c), the Φ_h phase of 18 changes into a new phase. Various thermal treatments (i.e., heating, and cooling with different rates from the smectic or isotropic phase; annealing below 66 °C) failed to regenerate the Φ_h phase. Most probably the Φ_h phase is kinetically difficult to obtain through thermotropic transitions due to its close proximity to the glass transition temperature of 18 ($T_g = 49$ °C). However, the Φ_h phase formed easily when the polymer 18 was reprecipitated from solution and heated above its glass transition temperature.

At 160 °C, 18 shows an inner ring due to $d_o = 55 (\pm 1.5)$ Å = d_{001} (at room temperature $d_o = 53$ Å) and an outer ring due to $d_1 = 26.5$ Å = d_{002} . Since $d_1/d_o = 2$, this phase is most probably a layered phase, i.e., s_A or s_C . The end-to-end length of the side group from Chart Ia (i.e., from H to H) is 34.8 Å. After including the van der Waals radii of hydrogen it becomes 37 Å. Therefore, the smectic phase should be based on a double layer as shown in parts c and d of Chart I. It is very probable that at high temperature the tapering of the side group disappears due to the coiling of the spacer and/or backbone (Chart Id). Additional experiments are required to discriminate between the s_A or s_C character of this mesophase.

Regardless of the thermal history of the sample, polymer 17 exhibits only a double-layer smectic phase, which appears to be of the same type as the high-temperature smectic phase of 18. The smectic layer periodicity of 17 after annealing at 120 °C is $d_o = 53 (\pm 1.0)$ Å = d_{001} . The end-to-end length of the side groups of 17 calculated in the same way as the one of 18 is 35.6 Å.

Polymer 19 exhibits an enantiotropic columnar hexagonal (Φ_h) phase that extends from the glass transition (48 °C) to its isotropization temperature (193 °C). As obtained by precipitation from solution, 19 has no long-range positional order, but it appears to possess short-range columnar order. However, once heated above its glass transition temperature and particularly above the endotherm at 126 °C it exhibits a Φ_h mesophase. This mesophase is characterized by $d_o = 57.4$ Å (strong) = d_{100}^{hex} , $d_1 = 33.3$ Å (very weak) = d_{110}^{hex} , and $d_2 = 28.5$ Å (very weak) = d_{200}^{hex} . The radius of the column is $R = 33.3$ Å and its diameter is $2R = 67$ Å. The length of the extended conformation of the molecular model corresponding to the planar tapered shape of the structural unit of 19 was calculated from the Si atom to the H of the end of the dodecyl tail, in the same way as in the calculation performed for the case of 18, and is 41.2 Å. After including the van der Waals radius of hydrogen this length becomes 42 Å. These data can be accommodated by a columnar hexagonal structure in which the columns are similar to those of Chart Ib. Since the extended conformation of the structural unit of 19 (42 Å) is much longer than the radius of the column ($R = 33.3$ Å), a column like that depicted in Chart Ib can be constructed only if the dodecyl tails of the mesogen are largely coiled on the surface of the column or strongly interdigitated between two neighboring columns. Only a contraction of the propyl

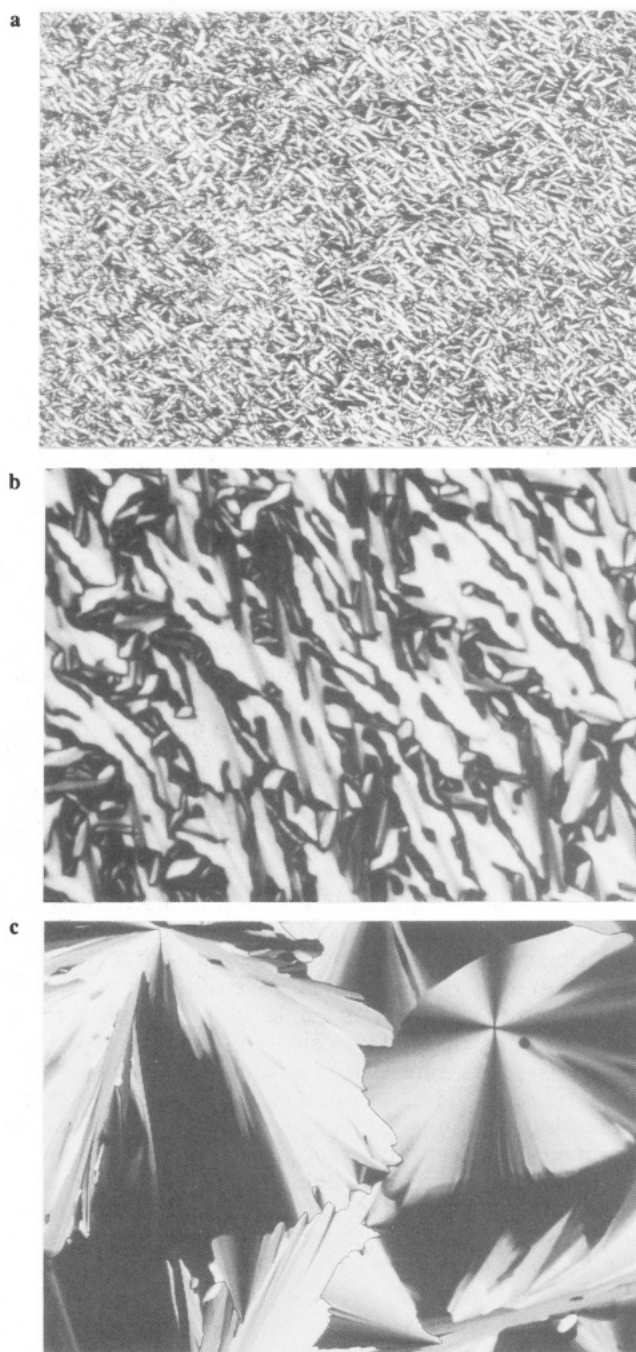


Figure 2. Representative optical polarized micrographs (65 \times) of the textures displayed by (a) the smectic phase of 17 after annealing at 168 °C for 30 min, (b) the smectic phase of 18 after cooling to 179 °C at 0.5 °C/min from the isotropic state, and (c) the hexagonal columnar phase of 19 after cooling to 180 °C at 5 °C/min from the isotropic state.

spacer is not sufficient to account for this difference.

Figure 2 presents some representative textures exhibited by the smectic phase of 17 (Figure 2a) and 18 (Figure 2b) and by the hexagonal columnar mesophase of 19 (Figure 2c). Upon slow cooling from the isotropic phase and annealing at 168 °C for 30 min, the texture of the smectic mesophase of 17 displays bâtonnets characteristic of a s_A phase (Figure 2a). Upon cooling from the isotropic phase at 0.5 °C/min and annealing at 179 °C for 10 min, polymer 18 forms first bâtonnets which merge into a focal conic texture (Figure 2b). This texture is also characteristic of a s_A mesophase. Finally upon being cooled at 5 °C/min from the isotropic phase to 180 °C, polymer 19 forms the texture in Figure 2c, which is representative of a hexagonal columnar mesophase exhibited by discotic liquid crystals.²⁵

Since this mesophase is generated very fast, i.e., is characterized by low viscosity, we believe it may indicate that the alkyl tails of the mesogens are more probably coiled on the surface of the column than interdigitated between two vicinal columns.

Definitive assignments of the nature of the smectic mesophase of 17 and 18 require additional X-ray scattering experiments performed on aligned samples. At the present time these experiments are not very important for our goals since we are mostly interested in the molecular design of polymers exhibiting hexagonal columnar mesophases.

So far, these preliminary X-ray scattering experiments have demonstrated that long alkyl tails in hemiphase mesogens of the type 14–16 favor the formation of hexagonal columnar mesophases, while short alkyl tails favor the formation of smectic double-layer mesophases. These data suggest that the length of the alkyl tail of the hemiphase mesogen has an important contribution to the overall shape of the mesogenic group. Short alkyl tails permit a rodlike conformation, which can be packed into a bilayer smectic phase. However, long alkyl tails generate a tapered shape, which is better accommodated in a cylindrical or columnar shape. At first sight these principles agree with those encountered in lipids or surfactants.²⁶ Single-chained lipids with large or small head group areas generated spherical and cylindrical micelles due to their cone or truncated cone shape. However, double-chained lipids with small head group or with large head group areas generate planar bilayers and flexible bilayers or vesicles due to their cylindrical or truncated cone shape.

To our knowledge, polymers 17 and 18 are the second examples of mesomorphic systems based on hemiphases that exhibit smectic mesophases. The first example was reported by Ringsdorf et al.⁶ We think that polymer 18 represents the first example of a hemiphase compound that exhibits a columnar hexagonal (Φ_h) to smectic (s) phase transition on heating. In most low molar mass biforked liquid crystals (i.e., rodlike mesogens containing two aliphatic tails at each end), both hexagonal columnar and smectic phases occur separated by a thermotropic transition.²⁷ However, in biforked low molar mass compounds, the columnar phase occurs at higher temperatures. In addition to 18 there are only a few polymers that exhibit a Φ_h to s phase transition. They are based on biforked mesogens.²⁸

Additional X-ray experiments are required to elucidate the structure of the hexagonal columnar mesophases displayed by these polymers. Nevertheless, the results presented in this paper suggest synthetic procedures for the molecular engineering of polymers exhibiting hexagonal columnar mesophases and containing both functionalized surfaces of their columns and channels penetrating through the column. Research on this line is in progress and will be reported in due time. Last, since liquid-crystalline polymers containing hemiphase mesogens are much easier to synthesize than the corresponding polymers containing disklike groups,²⁹ they may represent more suitable materials for the molecular understanding of polymers exhibiting hexagonal columnar mesophases.

Acknowledgment. Financial support from the National Science Foundation (MRG at CWRU and Polymer Program: DMR-86-19724) and the Office of Naval Research is gratefully acknowledged.

References and Notes

- (1) Percec, V.; Heck, J. *Polym. Prepr. (Am. Chem. Soc., Div. Polym. Chem.)* 1989, 30, 450.
- (2) Percec, V.; Heck, J. *J. Polym. Sci., Part A: Polym. Chem.* 1991, 29, 591.
- (3) Percec, V.; Heck, J. *Polym. Bull.* 1990, 24, 255.
- (4) Percec, V.; Heck, J. *Polym. Bull.* 1991, 25, 55.
- (5) Percec, V.; Heck, J. *Polym. Bull.* 1991, 25, 431.
- (6) Liu, C.; Ringsdorf, H.; Ebert, M.; Kleppinger, R.; Wendorff, J. H. *Liq. Cryst.* 1989, 5, 1841.
- (7) Demus, D. *Liq. Cryst.* 1989, 5, 75.
- (8) Malthête, J.; Levelut, A. M.; Tinh, N. H. *J. Phys. Lett.* 1985, 46, L-875.
- (9) Malthête, J.; Liebert, L.; Levelut, A. M.; Galerne, Y. C. R. *Acad. Sci., Ser. 2* 1986, 303, 1073.
- (10) Malthête, J.; Tinh, N. H.; Levelut, A. M. *J. Chem. Soc., Chem. Commun.* 1986, 1548.
- (11) Levelut, A. M.; Malthête, J.; Destade, C.; Tinh, N. H. *Liq. Cryst.* 1987, 2, 877.
- (12) Guillon, D.; Skoulios, A.; Malthête, J. *Europhys. Lett.* 1987, 3, 67.
- (13) Malthête, J.; Collet, A.; Levelut, A. M. *Liq. Cryst.* 1989, 5, 123.
- (14) Praefcke, K.; Kohne, B.; Gundogan, B.; Demus, D.; Diele, S.; Pelzl, G. *Mol. Cryst. Liq. Cryst. Lett.* 1990, 7, 27.
- (15) Chandrasekhar, S.; Ratna, B. R.; Sadashiva, B. K.; Raja, V. N. *Mol. Cryst. Liq. Cryst.* 1988, 165, 123.
- (16) Chandrasekhar, S.; Ranaganath, G. S. *Rep. Prog. Phys.* 1990, 53, 57.
- (17) For recent papers and reviews on hexagonal columnar mesophases obtained from disklike mesogens see: (a) Reference 16. (b) Ringsdorf, H.; Wüstefeld, R. *Philos. Trans. R. Soc. London*, A 1990, 330, 95. (c) Percec, V.; Cho, C. G.; Pugh, C. J. *Mater. Chem.* 1991, 217. (d) Percec, V.; Cho, C. G.; Pugh, C. *Macromolecules* 1991, 24, 3227. (e) The introduction to this paper reviews the field of polymers containing disklike mesogens: Percec, V.; Cho, C. G.; Pugh, C.; Tomazos, D. *Macromolecules*, submitted. (f) For a review on hexagonal columnar mesophases exhibited also by conventional flexible polymers, see: Ungar, G. *Polymer*, in press.
- (18) Ungar, G.; Feijoo, J. L.; Percec, V.; Yourd, R. *Macromolecules* 1991, 24, 953.
- (19) (a) Spegt, P.; Skoulios, A. *Acta Crystallogr.* 1963, 16, 301. (b) Godguin-Giroud, A. M.; Marchon, J. C.; Guillon, D.; Skoulios, A. *J. Phys. (Paris) Lett.* 1984, 45, 681. (c) Winsor, P. A. *Chem. Rev.* 1968, 68, 1. (d) Pershan, P. S. *J. Phys., Colloq.* 1979, 40, C3-423. (e) Forrest, B. J.; Reeves, L. W. *Chem. Rev.* 1981, 81, 1. (f) Friberg, S. *Naturwissenschaften* 1977, 64, 612. (g) Ringsdorf, H.; Schlarb, B.; Venzmer, J. *Angew. Chem., Int. Ed. Engl.* 1988, 27, 113.
- (20) Hahn, B.; Percec, V. *Macromolecules* 1987, 20, 2961.
- (21) K. Holnberg, K.; Hansen, B. *Acta. Chem. Scand.* 1979, B33, 410.
- (22) (a) Percec, V.; Keller, A. *Macromolecules* 1990, 23, 4347. (b) Keller, A.; Ungar, G.; Percec, V. In *Advances in Liquid Crystalline Polymers*; Weiss, R. A., Ober, C. K., Eds.; ACS Symposium Series 435; American Chemical Society: Washington DC, 1990; p 308.
- (23) Percec, V.; Pugh, C. In *Side Chain Liquid Crystal Polymers*, McArdle, C. B., Ed.; Chapman and Hall: New York, 1989; p 30.
- (24) Percec, V.; Tomazos, D.; Pugh, C. *Macromolecules* 1989, 22, 3259.
- (25) (a) Destade, C.; Foucher, P.; Gasparoux, H.; Tinh, N. H.; Levelut, A. M.; A. M.; Malthête, J. *Mol. Cryst. Liq. Cryst.* 1984, 106, 121. (b) Destade, C.; Gasparoux, H.; Foucher, P.; Tinh, N. H.; Malthête, J.; Jacques, J. *J. Chim. Phys. (Paris)* 1983, 80, 137. (c) Manlok, L.; Malthête, J.; Tinh, N. H.; Destade, C.; Levelut, A. M. *J. Phys. Lett.* 1982, 43, L641. (d) Tinh, N. H.; Malthête, J.; Gasparoux, H.; Destade, C. In *Liquid Crystals and Ordered Fluids*; Griffin, A. C., Johnson, J. F., Eds.; Plenum Press: New York, 1984; Vol. 4; p 1123.
- (26) Israelachvili, J. N. *Intermolecular and Surface Forces. With Applications to Colloidal and Biological Systems*; Academic Press: New York, 1986; p 256.
- (27) Destade, C.; Tinh, N. H.; Roubineau, A.; Levelut, A. M. *Mol. Cryst. Liq. Cryst.* 1988, 159, 163.
- (28) Achard, M. F.; Tinh, N. H.; Richard, H.; Mauzac, M.; Hardouin, F. *Liq. Cryst.* 1990, 8, 533.
- (29) (a) Kreuder, W.; Ringsdorf, H. *Makromol. Chem., Rapid Commun.* 1983, 4, 807. (b) Kreuder, W.; Ringsdorf, H.; Tschirner, P. *Makromol. Chem., Rapid Commun.* 1985, 6, 367. (c) Wenz, G. *Makromol. Chem., Rapid Commun.* 1985, 6, 577. (d) Ringsdorf, H.; Tschirner, P.; Hermann-Schönherr, O.; Wendorff, J. H. *Makromol. Chem.* 1987, 188, 1431. (e) Kranig, W.; Spiess, H. W.; Zimmermann, H. *Liq. Cryst.* 1990, 7, 123. (f) Ringsdorf, H.; Wüstefeld, R.; Zerta, E.; Ebert, M.; Wendorff, J. H. *Angew. Chem., Int. Ed. Engl.* 1989, 28, 914. (g) Kohne, B.; Praefcke, K.; Ringsdorf, H.; Tschirner, P. *Liq. Cryst.* 1989, 4, 165. (h) Fouquey, C.; Lehn, J. M.; Levelut, A. M. *Adv. Mater.* 1990, 2, 254.